ORGANIC LETTERS

2000
Vol. 2, No. 14
1995−1998

A Cavitand–Porphyrin Hybrid

Stephen D. Starnes, Dmitry M. Rudkevich,† and Julius Rebek, Jr.*

The Skaggs Institute for Chemical Biology and The Department of Chemistry, The Scripps Research Institute, 10550 North Torrey Pines Road, La Jolla, California 92037

jrebek@scripps.edu

Received April 11, 2000

ABSTRACT

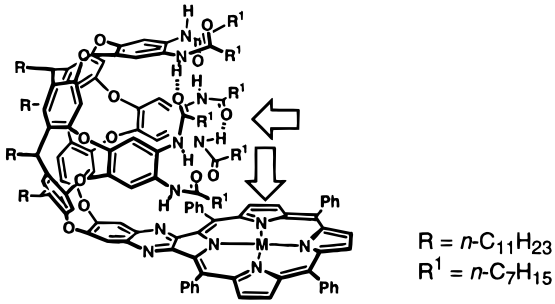

Host–guest complexes of a new open-ended cavitand show unprecedented stabilities. Simultaneous binding in the cavity and at the metalloporphyrin affects both the kinetics and the thermodynamics of caviplex formation.

Cavitands are synthetic structures with enforced, open-ended cavities that act as hosts for smaller molecular guests.[1] The host−guest complexes of self-folding cavitands **1** (Figure 1) show high kinetic stability, a consequence of the deep cavity and the seam of intramolecular hydrogen bonds. These bonds control the cavity's conformational dynamics and are ruptured during the uptake and release of guests.[2] The thermodynamic stabilities still remain low—binding involves the weakest of intermolecular forces (van der Waals and C−H/π interactions) and only the occasional hydrogen bond.

Here we introduce a porphyrin derivative that presents additional functionality and show that its metal complex can be brought to bear on guests held inside the cavitand. Caviplexes of unprecedented kinetic and thermodynamic stability are the result.[3]

The synthesis of the new structure **2** (Figure 1) takes advantage of the versatile diamine **3**, described earlier in the context of other nanoscale structures.[4] Condensation of **3** with porphyrin diketone **4**[5] in anhydrous toluene afforded the metal-free porphyrin in 43% yield (Scheme 1). Subsequent metalation with $Zn(OAc)_2$ in refluxing $CHCl_3$/MeOH readily gave **2** as the only product.[6] The simple Zn−porphyrin **5** was also prepared for comparison purposes.

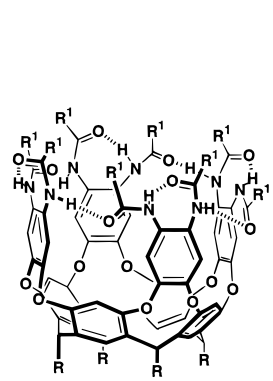

1 R = *n*-$C_{11}H_{23}$, R^1 = *n*-C_7H_{15}

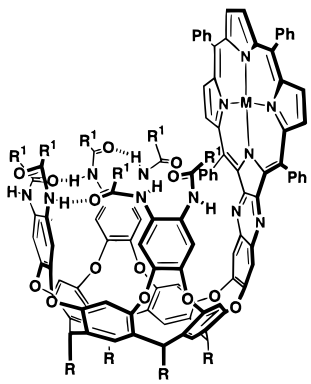

2 M = Zn, R = *n*-$C_{11}H_{23}$, R^1 = *n*-C_7H_{15}

Figure 1. Cavitands **1** and **2**.

† Also available for correspondence. Email: dmitry@scripps.edu.

(1) (a) Cram, D. J. *Science* **1983**, *219*, 1177−1183. (b) Cram, D. J.; Cram, J. M. *Container Molecules and their Guests*; Royal Society of Chemistry: Cambridge, 1994; pp 85−106. (c) Rudkevich, D. M.; Rebek, J., Jr. *Eur. J. Org. Chem.* **1999**, 1991−2005.

(2) (a) Rudkevich, D. M.; Hilmersson, G.; Rebek, J., Jr. *J. Am. Chem. Soc.* **1997**, *119*, 9911−9912. (b) Rudkevich, D. M.; Hilmersson, G.; Rebek, J., Jr. *J. Am. Chem. Soc.* **1998**, *120*, 12216−12225. (c) Ma, S.; Rudkevich, D. M.; Rebek, J., Jr. *Angew. Chem., Int. Ed.* **1999**, *38*, 2600−2602.

10.1021/ol0000859 CCC: $19.00
Published on Web 06/13/2000

Scheme 1

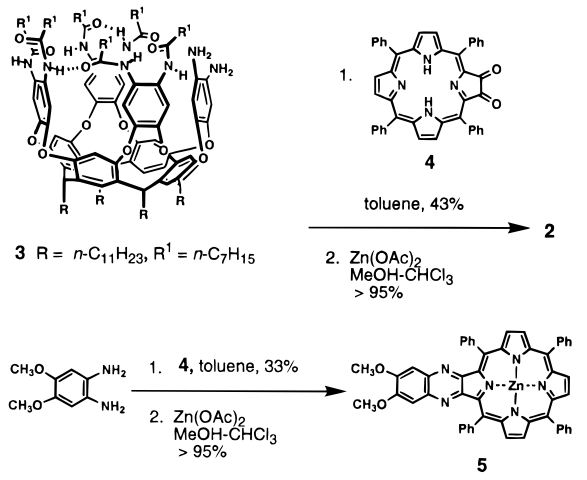

The C(O)-NH resonances of **2** are observed far downfield of 8 ppm in the ^{1}H NMR spectra ($CDCl_3$, benzene-d_6, toluene-d_8, etc.), and the corresponding IR spectrum shows hydrogen bonded N−H stretching absorptions at 3240 cm^{-1} (toluene). Accordingly, the secondary amides form a seam of intramolecular hydrogen bonds, and their arrangements are cycloenantiomeric: either clockwise or counterclockwise orientation of the head-to-tail amides is possible. The interconversion between the two enantiomers is fast on the NMR time scale (600 MHz, at ≥ 273 K) since the ^{1}H NMR spectrum indicates a structure having a plane of symmetry.

The internal cavity dimensions are estimated at 9 × 10 Å, and the distance between the cavity's bottom and the porphyrin's metal center is ∼14 Å. A series of amide-linked guests, **6**, **7**, **8a**−**e**, and **9a,b** (Figure 2), containing either adamantyl or pyridyl fragments or both were used in binding assays in toluene-d_8.[6] Neither adamantane **6** nor pyridine **7** gave evidence of kinetically stable binding to **2** at room temperature.[7] In contrast, only 0.4 equiv of adamantylpyridyl guest **9b** was needed to give new signals for the complex **2**·**9b** (Figure 3). *Both* adamantyl and pyridyl signals of the complexed guest are seen shifted upfield, and separate sets of signals for the free and bound host are apparent. Accordingly, bidentate 1:1 binding occurred, with the adamantyl fragment held within the cavity of **2** and the pyridine complexed to the metal of the porphyrin wall (Figure 4, left). The ^{1}H NMR spectrum of complex **2**·**9b** is rather broad at 295 K but sharpens as the temperature is lowered; at ≤ 280 K, sharp signals were observed. All amide N-H signals were now seen separately indicating that the interconversion between the cycloenantiomers within the complex is slow. In guest-free **2**, cycloenantiomers interconvert rapidly even at lower temperatures. Titration experiments with **2** and **9b** in toluene, using UV−vis spectroscopy, gave the association constant for complexation of 1.1 × 10^7 M^{-1} ± 10% ($-\Delta G^{295}$ = 9.5 kcal mol^{-1}; Figure 4, right).

The interaction between the Zn−porphyrin wall and pyridyl group in toluene was reasonably estimated from the titrations with **2** and **7** or **5** and **9b**, respectively, and it does not exceed $-\Delta G^{295}$ ∼6.0 kcal mol^{-1}. Accordingly, any additional energy of binding guests **8a**−**e** and **9a**,**b** should reflect a direct participation of the cavity (Table 1). Indeed, such cavity effects of $\Delta\Delta G^{295}$ = 1.5−3.5 kcal mol^{-1} were found for adamantylpyridines **8c**,**d** and **9b** where the bound

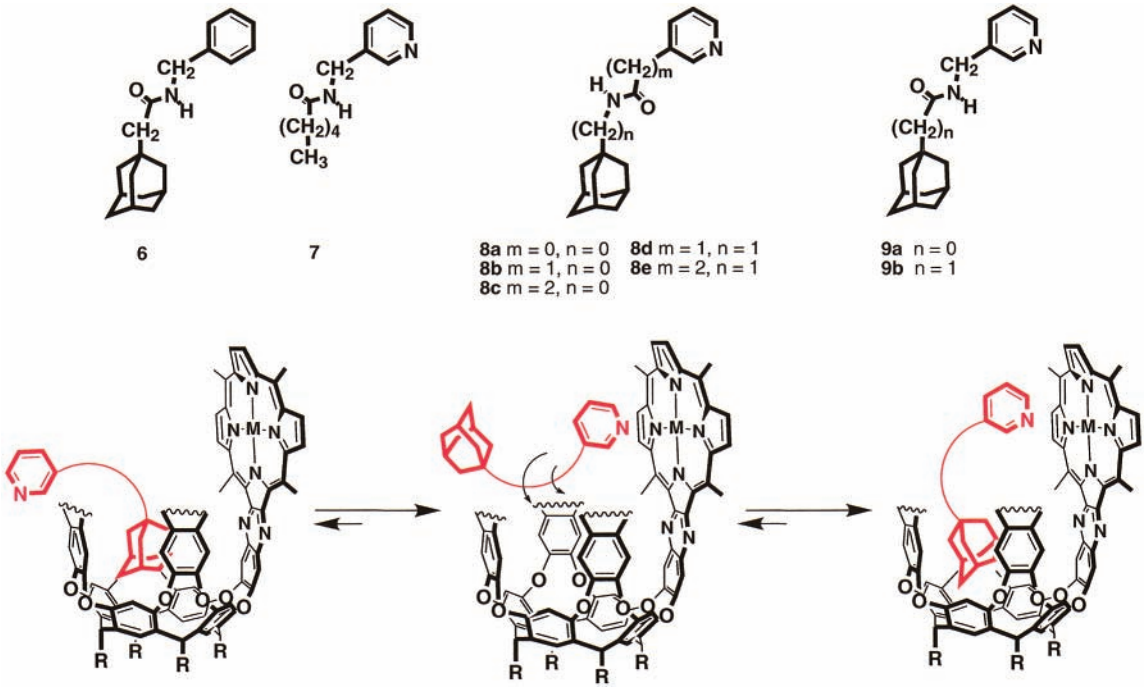

Figure 2. Guests **6**−**9** and schematic representation of bidentate binding in caviplex **2**.

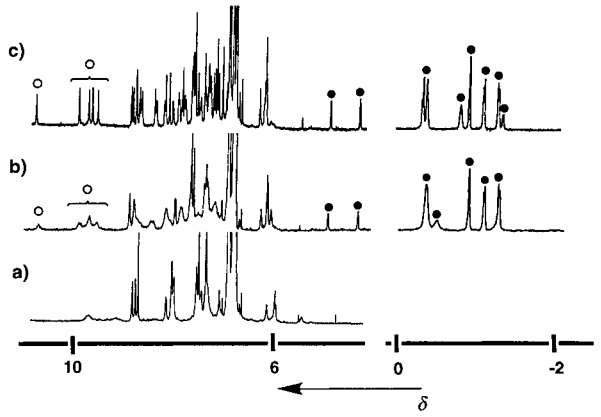

Figure 3. Downfield and upfield regions of the ^{1}H NMR spectra in toluene-d_8 (600 MHz): (a) guest-free cavitand **2** at 295 K; (b) caviplex **2·9b** at 295 K; (c) same as (b) at 273 K. The amide N−H signals are designated as ○ and the encapsulated **9b** signals are marked as ●.

Table 1. Association Constants (K_{ass}, M^{-1}) and Binding Energies ($-\Delta G$,^{295} kcal mol^{-1}) of Guests **6**−**9** by Porphyrins **2** and **5**[a,b]

complex	ln K_{ass}	$-\Delta G^{295}$	$\Delta\Delta G^{295}$ [d]
2 + **6**	[c]	[c]	
2 + **7**	10.3	6.0	0.0
2 + **8a**	10.5	6.1	0.1
2 + **8b**	11.8	6.9	0.9
2 + **8c**	13.6	7.9	1.9
2 + **8d**	12.9	7.5	1.5
2 + **8e**	12.0	7.0	1.0
2 + **9a**	9.5	5.6	−0.4
2 + **9b**	16.2	9.5	3.5
5 + **9b**	8.9	5.2	

[a] Determined by UV−vis in toluene at 295 K. [**2**] = 4.5 × 10^{-6} M, [**5**] = 4.5 × 10^{-6} M, guest concentration range 1.0 × 10^{-6} − 8.0 × 10^{-5} M. Error ±10%. [b] Data obtained from at least two independent experiments. [c] No visible complexation was detected by UV−vis in toluene at 295 K. No kinetically stable complex was detected at 295 K by ^{1}H NMR in toluene-d_8. At 273 K, ln K_{ass} = 5.0 and $-\Delta G^{295}$ = 2.7 kcal mol^{-1} were calculated from the ^{1}H NMR experiment in toluene-d_8. [d] $\Delta\Delta G^{295}$ = ($-\Delta G^{295}$ **2** + guest) − ($-\Delta G^{295}$ **2** + **7**).

fragments are separated by two methylenes and a secondary amide. This appears to be the optimal length; with the shorter guests **8a**,**b** and **9a** the cavity contributed less than 1 kcal mol^{-1}. Longer guest **8e** was somewhat in the middle ($\Delta\Delta G^{295}$ = 1.0 kcal mol^{-1}) (Table 1).[8]

In summary, a new type of cavitand with unique binding affinities is at hand. The presence of the metalloporphyrin wall opens the possibility of using these containers as catalytic vessels, as the flow of the substrate into and the product out of the cavity is expected to be rapid on the human time scale. The UV−vis spectral changes detected upon complexation suggest applications in analysis and sensing, and energy transfer from the porphyrin wall of cavitand **2** to an appropriate guest molecule can also be expected. These applications are currently underway.

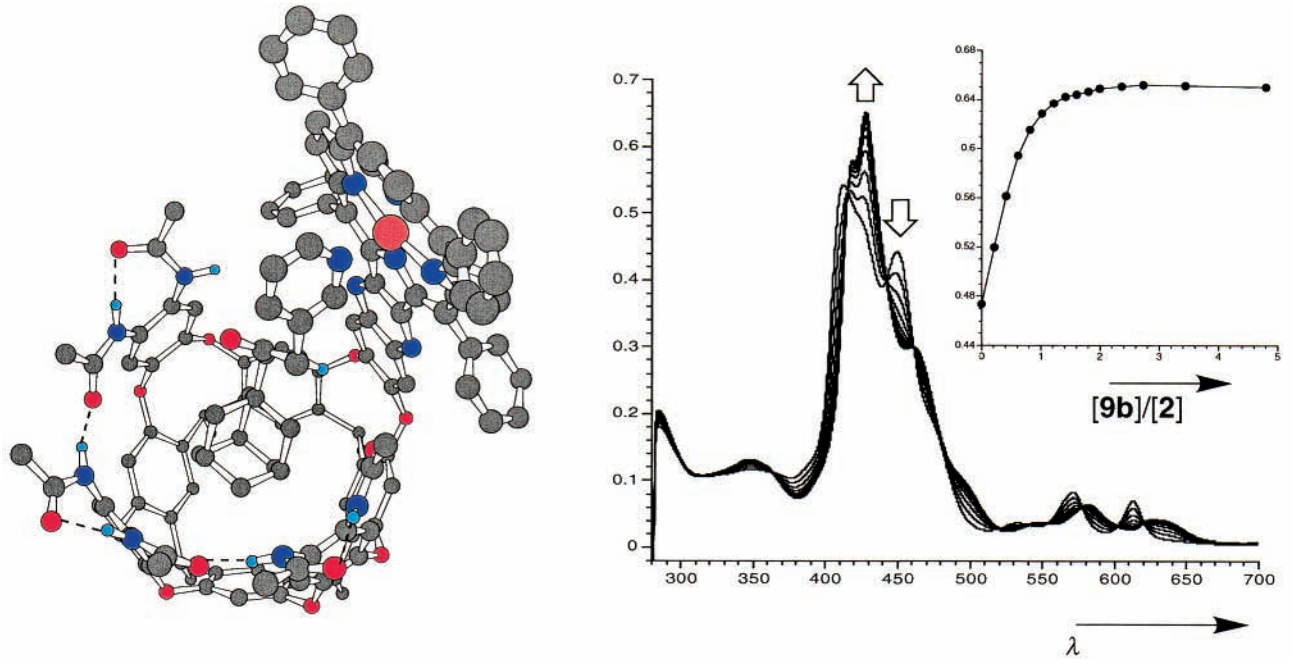

Figure 4. Left: energy-minimized structure of caviplex **2·9b**. Long alkyl chains and CH hydrogens have been omitted for viewing clarity. Right: portions of the UV−vis titration spectra with guest **9b** (toluene, 295 K). The Soret band of **2** at 412 nm shifted to 428 nm upon complexation. The inset represents the change in absorbance of **2** at 428 nm with varying molar equivalents of **9b**. [2] = 4.5 × 10^{-6} M, [**9b**] = 0.8 × 10^{-6} − 3 × 10^{-5} M.

Acknowledgment. We are grateful for financial support from the Skaggs Research Foundation and the National Institutes of Health. We thank Prof. Dr. F. N. Diederich for providing us with the curve-fitting program.

Supporting Information Available: Representative ^{1}H NMR spectra of compound **2** and complexes **2·9a** and **2·9b** at 273 and 298 K. UV/vis spectra of **2·8a**, **2·8b**, and **2·9b**. This material is available free of charge via the Internet at http://pubs.acs.org.

OL0000859

(3) Cyclodextrin−porphyrins: (a) Kuroda, Y.; Hiroshige, T.; Sera, T.; Shiroiwa, Y.; Tanaka, H.; Ogoshi, H. *J. Am. Chem. Soc.* **1989**, *111*, 1912−1913. (b) Kuroda, Y.; Ito, M.; Sera, T.; Ogoshi, H. *J. Am. Chem. Soc.* **1993**, *115*, 7003−7004. Steroid-capped porphyrins: (c) Bonar-Law, R. P.; Sanders, J. K. M. *J. Am. Chem. Soc.* **1995**, *117*, 259−271. (d) Bonar-Law, R. P.; Sanders, J. K. M. *J. Chem. Soc., Perkin Trans. 1* **1995**, 3085−3096. Calixarene−porphyrins: (e) Rudkevich, D. M.; Verboom, W.; Reinhoudt, D. N. *Tetrahedron Lett.* **1994**, *35*, 7131−7134. (f) Rudkevich, D. M.; Verboom, W.; Reinhoudt, D. N. *J. Org. Chem.* **1995**, *60*, 6585−6587. (g) Nagasaki, T.; Fujishima, H.; Takeuchi, M.; Shinkai, S. *J. Chem. Soc., Perkin Trans. 1* **1995**, 1883−1888. Glycoluril−porphyrins: (h) Reek, J. N. H.; Rowan, A. E.; Crossley, M. J.; Nolte, R. J. M. *J. Org. Chem.* **1999**, *64*, 6653−6663. (i) Elemans, J. A. A. W.; Claase, M. B.; Aarts, P. P. M.; Rowan, A. E.; Schenning, A. P. H. J.; Nolte, R. J. M. *J. Org. Chem.* **1999**, *64*, 7009−7016. Cyclophane−porphyrins: (j) Benson, D. R.; Valentekovich, R.; Knobler, C. B.; Diederich, F. *Tetrahedron* **1991**, *47*, 2401−2422. Cyclic arrays of metalloporphyrins: (k) Anderson, S.; Anderson, H. L.; Bashall, A.; McPartlin, M.; Sanders, J. K. M. *Angew. Chem., Int. Ed. Engl.* **1995**, *34*, 1096−1099. Here, high kinetic and thermodynamic stability of the complexes was demonstrated, however, through multiple ligand−metal interactions.

(4) Tucci, F. C.; Renslo, A. R.; Rudkevich, D. M.; Rebek, J., Jr. *Angew. Chem., Int. Ed.* **2000**, *39*, 1076−1079.

(5) Beavington, R.; Rees, P. A.; Burn, P. L. *J. Chem. Soc., Perkin Trans. 1* **1998**, 2847−2851.

(6) All compounds synthesized were characterized by FTIR, high-resolution ^{1}H and ^{13}C NMR spectroscopy, and high-resolution mass spectrometry. Pure amides **8a**−**e** and **9a**,**b** were obtained as colorless solids in 75−90% yields after crystallization, using textbook procedures of peptide chemistry. Complexation experiments were performed on a Bruker DRX-600 spectrometer (600 MHz) in toluene-d_8 and on a Perkin-Elmer UV−vis Lambda 12 spectrophotometer. Molecular modeling was performed using the Amber* force field in the Macromodel 5.5 program: Mohamadi, F.; Richards, N. G.; Guida, W. C.; Liskamp, R.; Lipton, M.; Caufield, C.; Chang, G.; Hendrickson, T.; Still, W. C. *J. Comput. Chem.* **1990**, *11*, 440−467.

(7) Slow exchange between the free and complexed adamantane guests **6**, **8a**−**e**, and **9a**,**b** was, however, detected at ≤ 273 K (in toluene-d_8). See also ref 4.

(8) In a competition ^{1}H NMR experiment with caviplexes of **2**, guest **9b** replaced guest **8d** within a few minutes (toluene-d_8, 273 K).